Composite Structures, Volume 166, 15 April 2017, Pages 184-192, DOI:10.1016/j.compstruct.2017.01.029

Bearing Damage Characteristics of Fibre-reinforced Countersunk Composite Bolted Joints Subjected to Quasi-static Shear Loading

Hamed Yazdani Nezhad[1], Brian Egan[2], Fiachra Merwick[3], Conor T. McCarthy[*]

Bernal Institute, Irish Centre for Composites, Research School of Engineering, Faculty of Science & Engineering, University of Limerick, Ireland

[1]Now at Enhanced Composites and Structures Centre, School of Aerospace, Transport and Manufacturing, Cranfield University, College Road MK43 0AL, United Kingdom

[2] Now at Wood Group Kenny, Galway Technology Park, Parkmore, Galway, Ireland

[3]Now at BASE Ltd. UK, The Innovation Centre, Northern Ireland Science Park, Queen's Road, Queen's Island, Belfast, BT3 9DT, Northern Ireland

Abstract

This paper studies the progression of damage in carbon fibre-reinforced polymer (CFRP) countersunk composite bolted joints (CBJs) with neat-fit clearance, subjected to quasi-static loading. Damage mechanisms, comprising of fibre buckling and breakage, matrix damage, shear damage and inter-laminar delamination within the CFRP composite parts of the joints have been studied. Load-displacement curves, X-ray and optical microscopic images in single- and three-bolt CBJs were used to investigate damage and deformation characteristics. The observations were then employed to further investigate the type of failure and the extent of damage. The evolution of damage within the composite parts was correlated to the failure characteristics of the joints: It was found that the type and extension of damage is strongly correlated with the ultimate failure load point of the joint in single-bolt CBJs. A combined inter/intra-laminar damage consisting of fibre cluster breakage, extensive fibre buckling, debonding and delamination was observed at the ultimate failure load. This study was then extended to three-bolt CBJ where damage surrounding each bolt and its corresponding failure load was strongly correlated: The final study showed that the ultimate failure point in single-bolt CBJ and the first-bolt-failure point in three-bolt CBJ correspond to the composite plies undergoing intra-laminar damage with the size reaching to the edge of the countersunk head. This damage developed extensively through the thickness of the composite parts underneath the countersink, and in the direction opposite to the loading direction. Outside the countersunk head, debonding and delamination were found to be the dominant damage driving mechanisms. Finally, a new design rule has been proposed to predict the response of multi-bolt joints (damage area and failure load) by using the response in single-bolt CBJ as an initial baseline.

Keywords: composite bolted joint; intra-laminar damage; fibre breakage; delamination; debonding; fastener failure

[*]Corresponding author: conor.mccarthy@ul.ie, Tel: +353 61 234334

1. Introduction

The mechanical response of composite countersunk bolted joint (CBJ) to various loading conditions has recently been an area of significant interest within intense ongoing procedures [1-8]. The purpose of this paper is to accurately understand underlying damage mechanisms in quasi-statically loaded CBJ structures when subjected to shear loading, and to provide an in-depth design basis for joint sizing applications. Failure can arise due to a variety of composite damage mechanisms along with fastener failure. Intra-laminar damage (e.g. matrix cracking, fibre failure, fibre-matrix debonding and intra-laminar delamination) and inter-laminar delamination mainly contribute to the damage characteristics of CBJs. However, a detailed analysis of the contribution of each mechanism in damage characteristics is not clear, i.e. which mechanisms mainly contribute to the joint strength reduction and what damage density each mechanism reaches at the ultimate failure. This is of particular interest to industry and designers as several numerical and experimental researches have shown that ply damage contributes to significant reduction in strength [1, 2, 9, 10] which, in the case of CBJs, may occur before fastener failure [1, 2]. The type and extent of dominant mechanisms also change as a function of loading direction. The region over which damage is occurring also depends on the bolt clearance in CBJs as was studied in [1, 11, 12]. However, in this paper we study the type of damage and extension in neat-fit clearance CBJs under shear loads. These experimental studies have led to development of a new design rule to predict the damage response in a multi-bolt CBJ based on development of damage area and linear superposition of failure load.

2. Experiments

2.1. Test setup

The test case under consideration is a quasi-static uniaxial bearing tests of a countersunk head bolted joint. The test coupons are from a quasi-static experimental test series carried out as part of the EU FP7 MAAXIMUS project [13] at Irish Centre for Composites Research at the University of Limerick. Figure 1(a) shows an annotated view of a typical single-lap single-bolt specimen in the displacement controlled uniaxial testing rig. A schematic of the joint geometry, including dimensions, is also shown in Figure 1(b). The bolt region in the top laminate is called CSK-L, referring to the countersunk laminate, while that in the lower (non-countersunk) laminate is denoted NCSK-L. The benchmark case featured a 2.125 mm thick laminate consisting of 17 0.125mm thick ply layups. The fastener is made from aerospace grade titanium alloy Ti-6Al-4V. The layup was considered for the fuselage joint analyses, designed for regions of low axial loading with an unsymmetrical stacking sequence of $+45/90/-45/0_3/\mathbf{-}45/0/90/0/\mathbf{+}45/0_3/-45/90/+45$ [13].

The countersunk bolts have a diameter of 4.8mm and a 130˚ countersunk head, are secured with steel nuts. A full description of the quasi-static experimental test series is given in [13, 14]. A loading rate of approximately 0.03 mm/s was used, and was sufficiently slow to yield a quasi-static result according to [15].

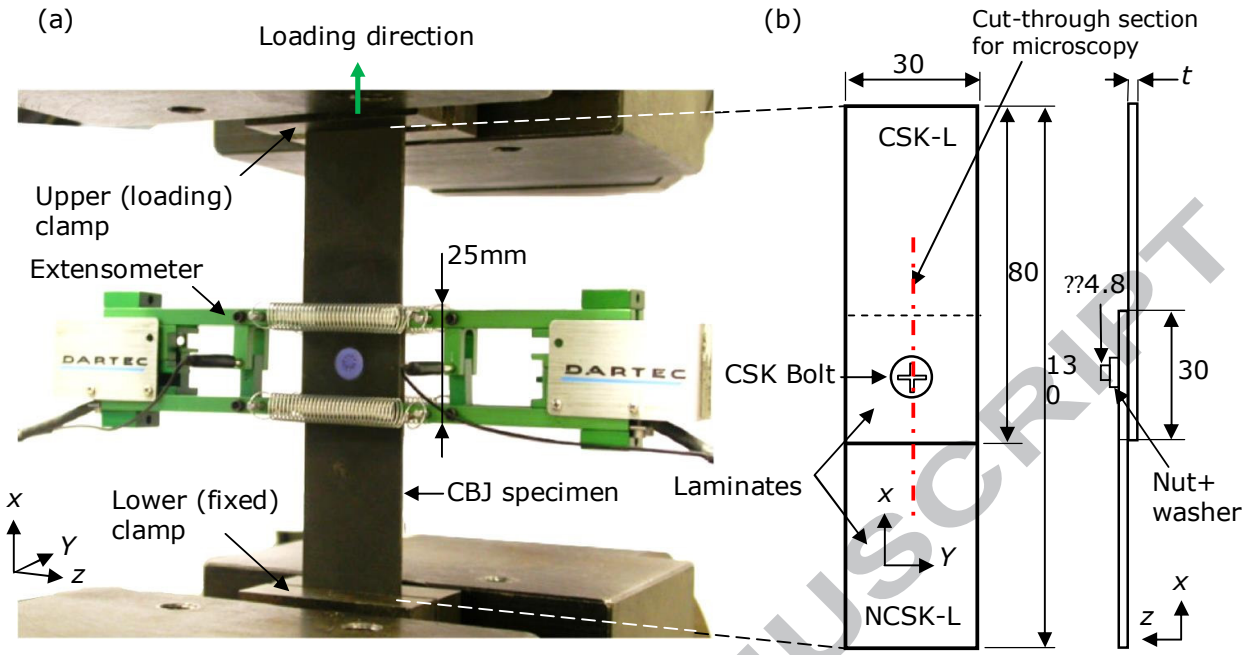

Figure 1: (a) CBJ test setup with extensometer [13], (b) single-lap single-bolt specimen geometry (all dimensions in mm)

As seen in Figure 1, a 25mm gauge length extensometer was used to capture relative displacement between the two laps of the CBJ specimen, CSK-L and NCSK-L. For three-bolt CBJs with a similar setup to that shown in Figure 1, digital image correlation (DIC) technique was used, instead of an extensometer, to measure extension at the end of the overlap region between the two laps, which served to eliminate the effect of machine stiffness on the experimental load-displacement data by allowing non-contact displacement on the specimen.

2.2. X-ray measurement

Non-destructive inspection of the CBJ specimens was carried out using X-ray scanning by means of an MI Faxitron machine and a NTB EZ240 scanner. The software used for controlling and viewing results was the iX-Pect EZ Version 1.2.7.37 software. The scanning speed of the scanner was set at 4 mm/sec, with an integration time of 20 milliseconds. The resolution of the image was 0.08 mm. Average scan time was approximately 15 seconds per joint side. A dye penetrant, di-iodomethane, was used to clearly highlight the damaged areas of the joint.

2.3. Optical microscopy

Optical images of the CSK-L damage area were captured using optical microscopy. The samples were initially cut, after X-ray measurements, to the required size so that they could be mounted in an epoxy resin. Upon curing of the resin, the samples were then ground down, by approximately 2mm, to reach the middle plane of the joint, shown by a dashed line in Figure 1(b), using a Phoenix 4000 polisher/grinder. The samples were then polished to a high degree of surface finish (Ra=0.2µm), to ensure scratches from the grinding

procedure were not visible in the images. The microscopy was conducted on an Olympus BX50 microscope. Images, at a magnification of 50X, were then taken at points of interest for each sample.

3. Experimental results

3.1. Single-bolt CBJ results

3.1.1. Damage development in single-bolt CBJ

In the quasi-static tests of the CBJ specimens, fastener pull-through, fastener failure and bearing damage were observed as final failure modes. Figure 2 shows the single-bolt CBJ failed by a combination of the bearing failure and fastener pull-through. Extensive bearing damage was observed in all tests until very late in the loading history prior to fastener failure. Some fibre-matrix cracking/debonding can be observed in NCSK-L close to the composite-nut interaction (see inset to Figure 2). However, the main source of damage in the joints was extensive bearing damage at the countersunk hole, which occurred prior to final catastrophic failure. This was to be expected as the joints were designed to initially fail in bearing [15]. The dashed line C-C represents the section where cut through CSK for microscopic studies presented later.

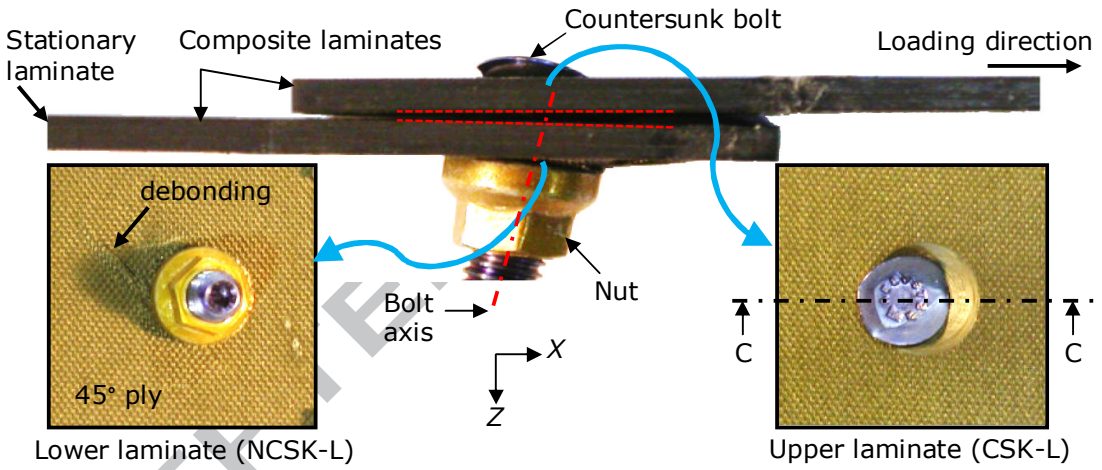

Figure 2: Combination of bearing and bolt failure in single-bolt CBJ. Dashed line C-C represents cut-through section for microscopic studies

3.1.2. Load-extension curves

Load-extension curves obtained from tensile bearing testing of two single-bolt CBJs are shown in Figure 3. Two joints showed similar trends. The main features are identified as primary, secondary and tertiary stiffness (all labelled in Figure 3). Test data obtained from the points and the slopes in the primary, secondary and tertiary regions are summarised in Table 1. The primary stiffness is due to sticking caused by friction between the laminates. The curves in Figure 3 present identical primary stiffness. Point A in Figure 3 is denoted at the end of this region, at which the primary stiffness drops to secondary stiffness. This drop is attributed to the sticking-to-slipping mechanism, and subsequent matrix damage. The value of the secondary stiffness shown in Table 1 has been obtained from the average of the two slopes between points A and B. After point B, a bound of ~1kN difference is observed between tests 1 and 2 at an equal extension. This

difference can be due to inherent differences occurring in assembly of the joint such as fastening pre-load. The pre-load has direct effect on friction coefficient between the CSK-L and NCSK-L surfaces in contact, and thus has a direct effect on the shear load. Tertiary stiffness is then obtained from the average of the two slopes between point B and the ultimate failure point 'C'.

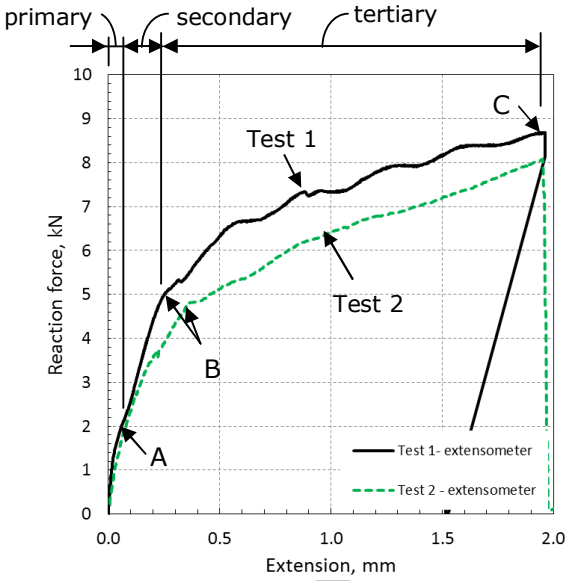

Figure 3: Load-extension behaviour of the single-bolt joints in single-lap CBJs

As defined in [15], bearing stress, $\sigma_{br} = P/(d.t)$ for a single-bolt joint, where P is the measured load, d is the hole diameter (4.8 mm) and t is the thickness of the countersunk (upper) laminate (e.g. 2.125 mm). According to the test data, the 2% offset bearing strength and the ultimate strength can be measured as 552.7 MPa and 816.7 MPa, corresponding to approximately 5.6kN and 8.3kN joint load, respectively. The drop from the primary stiffness to the secondary one at point A is approximately 60%. The drop from the primary and secondary stiffness to the tertiary one is very significant, > 90%. However, the CBJ extension is the highest in the tertiary region. This is attributed to the CSK hole elongation as a result of the compressive bearing damage to be discussed in the following section.

Table 1: Representative test data for single-bolt CBJ based on extensometer data

Test No.	Stiffness, kN/mm			Ratio of stiffnesses, %		Load (kN) & extension (mm) at points		
	Primary (O-A)	Secondary (A-B)	Tertiary (B-C)	Secondary/primary	Tertiary/primary	A	B	Ultimate failure point (C)
1	57.1	17.4	1.3	30	2.3	2.0 & 0.04	4.9 & 0.2	8.7 & 1.9
2	49.9	24.0	3.0	48	6	2.0 & 0.04	4.6 & 0.3	8.0 & 1.9

3.1.3. Visualisation of damage

Figure 4 shows the extent and type of damage in the single-bolt CBJ. The region was sectioned from section C-C shown in Figure 2. X-ray measurement from the top of the laminate (Z-direction) is presented in

Figure 5, showing the image for CSK and NCSK parts at joint extension of approximately 2 mm, where ultimate failure occurred (the ultimate strength is 816.7MPa). Hole elongation is evident in CSK due to compressive bearing damage, but no apparent elongation was observed in NCSK-L. The evident elongation in CSK is attributed to further compressive deformation introduced by the countersunk head of the bolt to the CSK material and area that has already been reduced due to insertion of the countersunk (hole elongation in Figure 5 is 15% at the joint maximum load.). The joint is orientated with the 0˚ fibre direction coinciding with the loading direction. Two major damage regions are identified in the X-ray image: 'dark' and 'bright' representing regions, respectively, with extensive and mild damage. The region with the near-surface damage (surrounded by the solid line) is not sharply captured in the X-ray image as opposed to the *dark* region within the dashed line where damage occurs within the bulk of the laminate. Damage beyond the countersunk region is attributed to the surface damage, and occurred by the bolt head crushing into the laminates and friction between the CSK and NCSK parts. This is consistent with the optical observations in Figure 4 where beyond the edge of the dark region surface damage, and not the bulk damage, is dominant.

The bearing damage in the microscopic image of Figure 4 is seen to consist of combined inter/intra-laminar damage to include fibre breakage and buckling under compressive load from the bolt, matrix damage, fibre-matrix debonding and delamination. The locations of interest are magnified in regions (1) to (5). Region (1) shows the furthest right-hand side of CSK-L where no damage is observed, expected due to having no contact with the bolt. Fibre buckling and breakage is observed in regions (2), (3) and (4) where the compressive stress was introduced by the fastener. Region 5 is located further from these local regions, where inter-laminar delamination occurred between plies 6 and 7, from bottom, in this region between (0˚ and 45˚ fibre orientations). This delamination follows from the combined damage seen in region (3). In region (5) an extensive fibre-matrix debonding occurs in the bottom (45°) ply. Transverse matrix damage is also visible. No in-plane or delamination damage was observed in the regions extending beyond region 5.

As seen in Figure 4 and Figure 5, X-ray has not captured damage *beyond* the countersunk edge which consists of debonding and delamination with no indication of fibre breakage. However, *within* the countersunk edge and also within the X-ray dark area, the combined damage occurred consisting of significant fibre buckling and breakage.

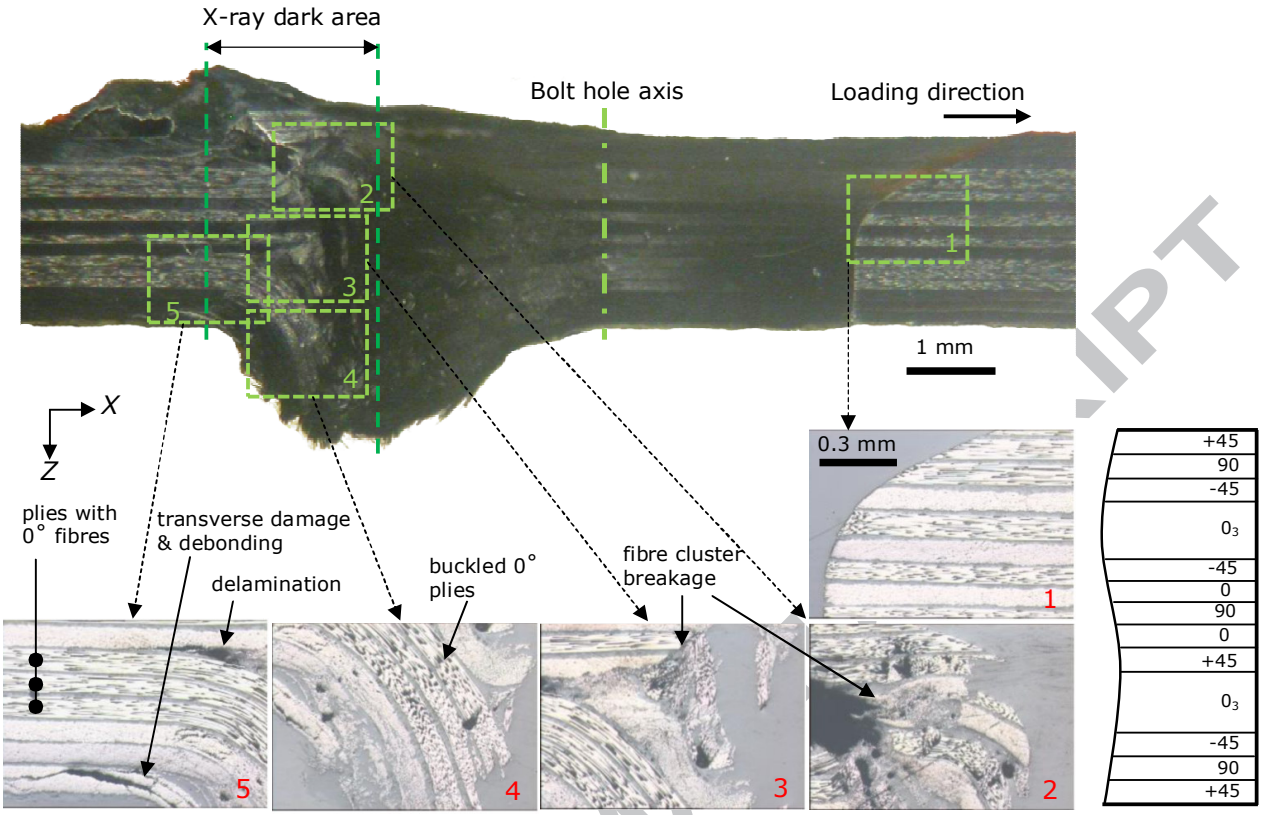

Figure 4: Damage in single-bolt CBJ's CSK

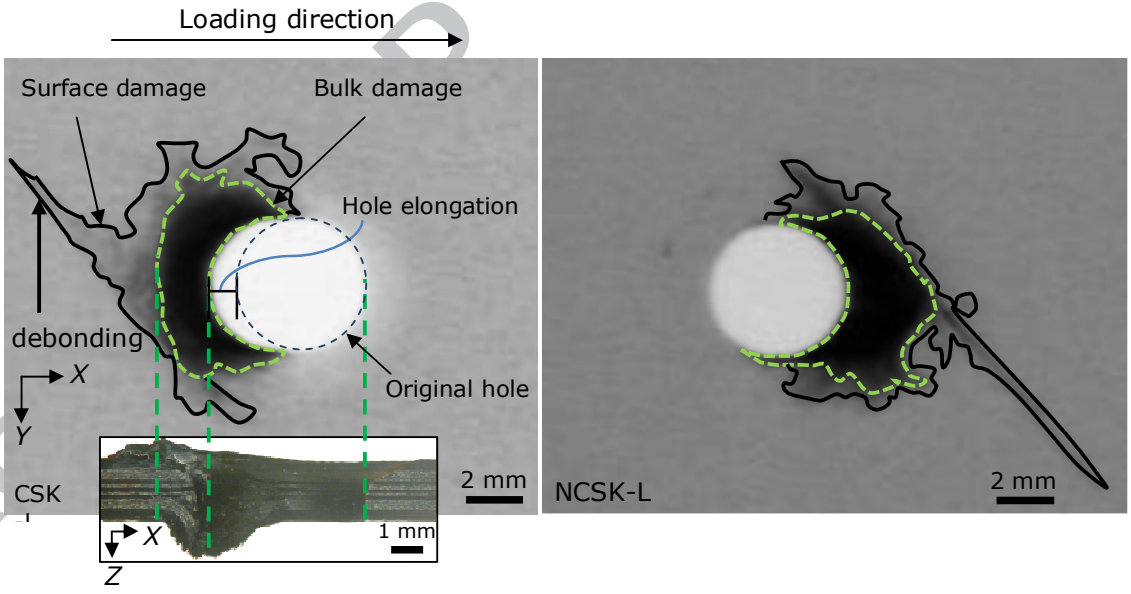

Figure 5: X-ray image of single-bolt CBJ (inset: optical image taken from Figure 4)

3.2. Three-bolt CBJ results

3.2.1. Damage development in three-bolt CBJ

Figure 6 shows the three-bolt CBJ after failure in which bolt failure is the final dominant failure mechanism. Note that the third bolt in the figure also failed but was not fully separated from the joint. Two bolts closest to the loading edge end (bolts 1 and 2) failed after significant bearing damage development.

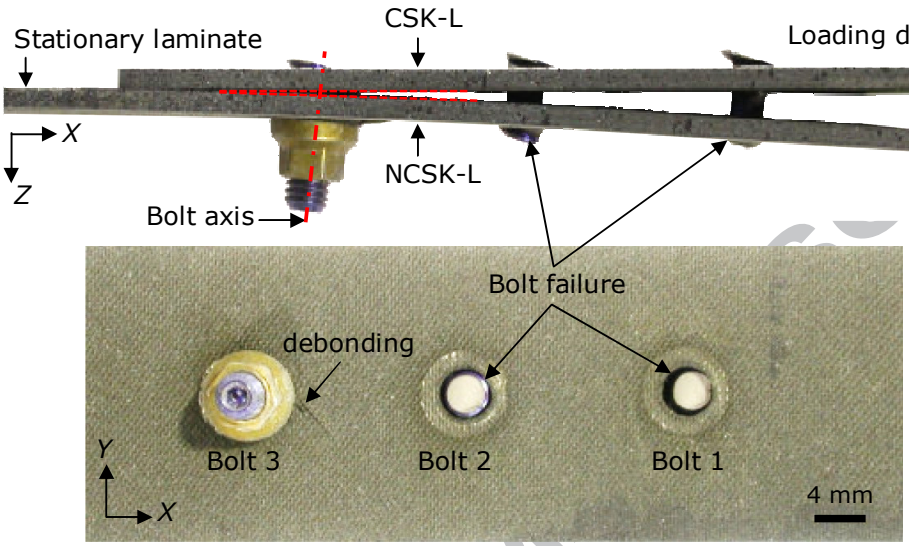

Figure 6: Combination of bearing and bolt failure in three-bolt CBJ

3.2.2. Load-extension curves

Figure 7 presents the load-extension response of the three-bolt CBJ. One curve from the single-bolt CBJ was also included in the figure for comparison. The dominant *final* failure in three-bolt CBJs was bolt failure promoting fastener pull-through. Bolt failure in multi-bolts is attributed to high shear load transfer [2]. Two tests show consistent peak load and equal drop in load level when bolts 1, 2 and 3 failed one after another. As seen in Figure 7, load carrying capacity of the last unfailed bolt (i.e. bolt 3) drops to 9.7kN, close to and slightly higher than that for the single-bolt CBJ which failed at 8.3kN. Thus, the three-bolt CBJ with its last bolt performs approximately the same as the single-bolt CBJ.

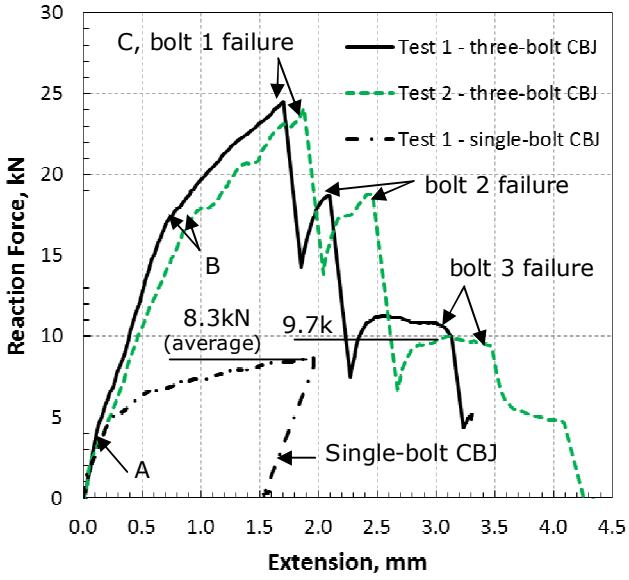

Figure 7: Load-extension behaviour of three-bolted joints extensometer data

Test data featuring salient points and stiffnesses at three significant load levels are also identified for the three-bolt CBJ before bolt 1 fails, presented in Table 2. Compared to the single-bolt case, bolt 1 failure in the three-bolt CBJ has occurred at approximately the same and slightly lower extension (at point C) and hole elongation. Reduction from the primary stiffness to the secondary one is 43% in the three-bolt CBJ, which is smaller than the reduction percentage in the single-bolt CBJ (60% reduction) due to the presence of other bolts stiffening effect. This is also the case for the reduction percentage in the tertiary regime which is 80% while it was 96% in the single-bolt one (see Table 1).

Surprisingly for the three-bolt CBJs examined in this work, the ultimate loads corresponding to fastener failure are 24.3kN, 18.7kN and 9.7kN, respectively for bolt 1, 2 and 3 failure. The peak load for the single-bolt CBJ was 8.3kN. Thus, the ratios of three-bolt ultimate failure loads to the single-bolt one are 2.9, 2.3 and 1.2 respectively. These values are not far from 3, 2 and 1, meaning that the ultimate loads increase proportionaly with the increasing number of bolts.

Table 2: Representative test data for three-bolt CBJ before bolt 1 failure

Test No.	Stiffness, kN/mm			Ratio of stiffnesses, %		Load (kN) & extension (mm) at points		
	Primary (O-A)	Secondary (A-B)	Tertiary (B-C)	Secondary/primary	Tertiary/primary	A	B	Ultimate failure point (C)
1	37.8	22.9	7.5	61	20	3.8 & 0.1	17.0 & 0.7	24.3 & 1.7
2	36.8	19.7	7.4	54	20	3.7 & 0.1	17.0 & 0.9	24.0 & 1.9

3.2.3. Visualisation of damage

Figure 8 presents the optical images from cross-section of the regions surrounding holes 1 and 2 in the three-bolt CBJ. It can clearly be seen that the topology and type of damage is not uniform throughout the

three-bolt joint, however, the images highlight the occurrence of in-plane damage as the dominant mechanism. The region surrounding hole 3 was severely damaged and could not provide any meaningful results, and so was not presented. For comparison, the X-ray image of the three-bolt CBJ is shown in Figure 9.

Severe buckling of 0° plies under compressive load is apparent in the three-bolt CBJ shown in Figure 8. For the single-bolt case (Figure 4), the 0° plies were also buckled in compression when the peak load was taken up to 8.3kN. Hence, assuming that in-plane damage is dominant, two simple statements can be derived for the CBJs examined here: 1- fibre buckling and breakage dominantly determine the load where ultimate failure occurs, and 2- 0° fibre buckling and breakage is present when the peak load ≥ 8.3kN.

Figure 8 also shows delamination followed by slight transverse matrix damage between 0° and 45° plies (in mid to bottom plies) as was also observed in single-bolts (6^{th} and 7^{th} plies from bottom in Figure 4). Similar to the single-bolt CBJ, the region where delamination occurred was not captured inside the X-ray dark region and neither the fibre-matrix debonding occurred at the bottom plies.

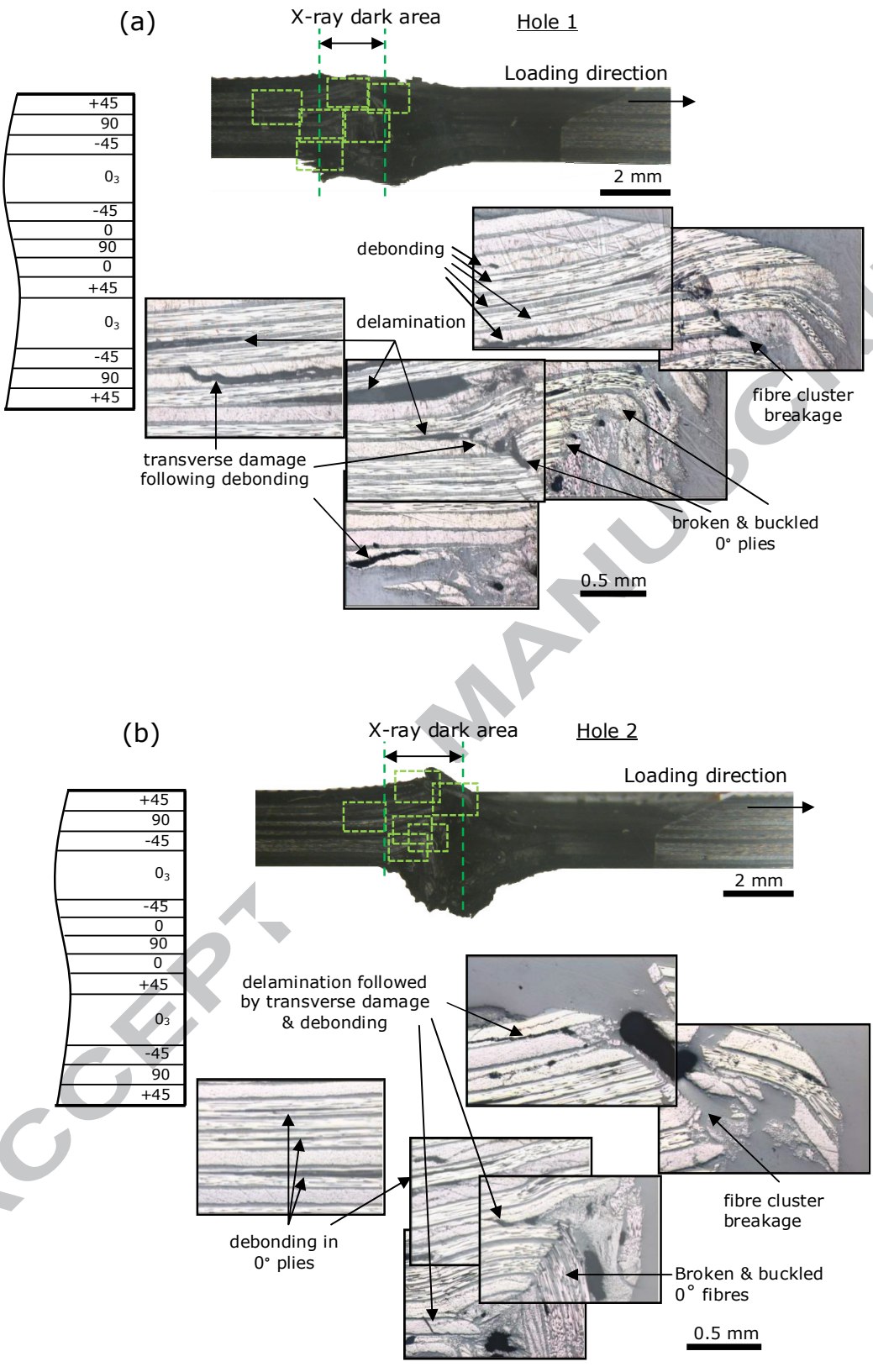

Figure 8: Damage in three-bolt CBJ's CSK; (a) Hole 1, (b) Hole 2

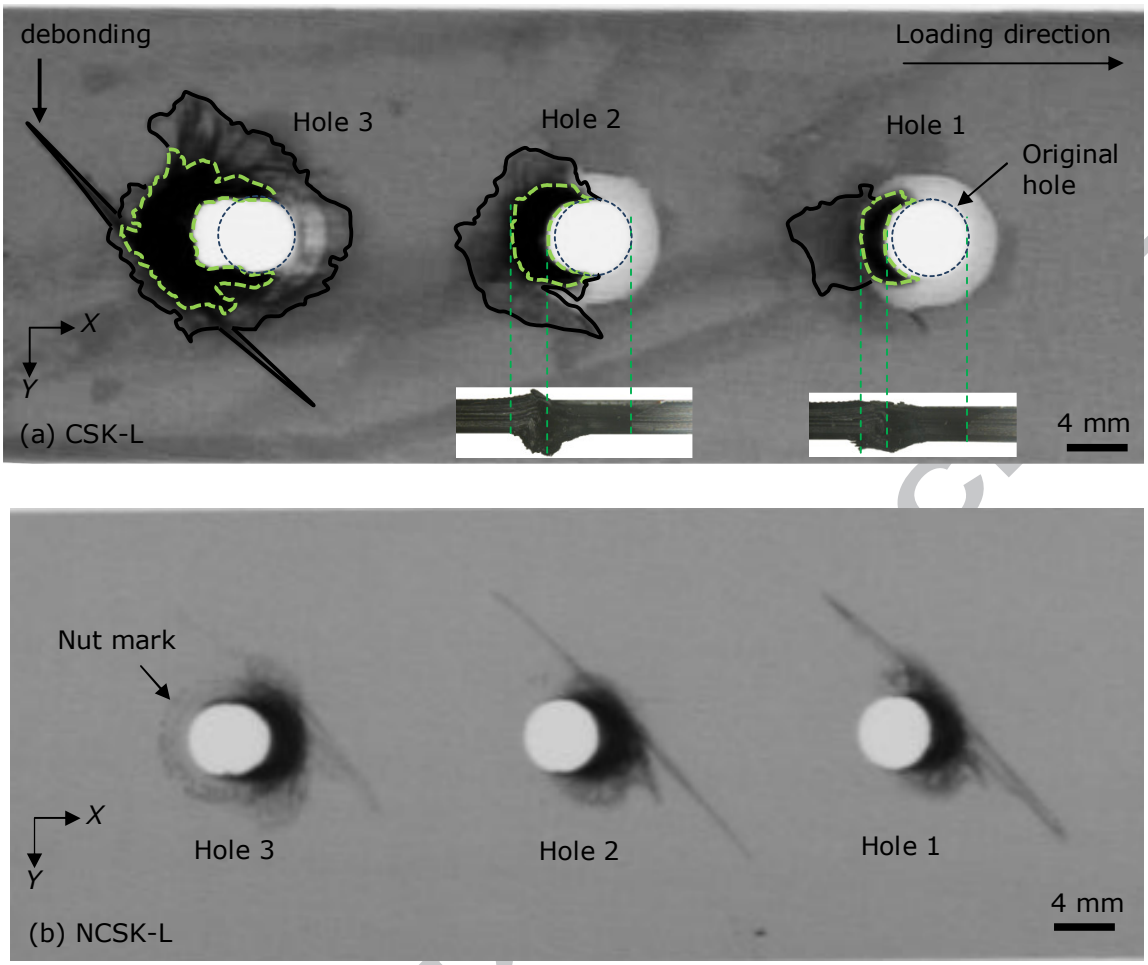

Figure 9: X-ray image of three-bolt CBJ using X-ray, (a) CSK-L, (b) NCSK-L

As seen in Figure 9(a), damage area in the CSK part is largest at Hole 3 and smallest at Hole 1, while damage at each bolt-hole in the NCSK laminate in Figure 9(b) is almost identical. This difference in damage area is attributed to the presence of countersunk head crushing into the top surface of the CSK laminate, as was clearly observed during testing. This observation is in stark contrast to what is observed in protruding head bolted joints, where damage is anti-symmetric, meaning that damage at Hole 1 in one joint member is normally equal to damage at Hole 3 in the opposite joint member [16, 17]. This loss of anti-symmetry means that countersunk bolted joints must be analysed fully at each bolt-hole, and that simplifying extrapolations derived from single-bolted joint tests must be used with caution. We thus now offer a new method to predict the damage growth in CSK joints based on the concept of damage areas.

Consider the damage development outlined in Figure 10 in conjunction with the joint load displacement curve in Figure 7. As the joint loads up to the first significant failure event at 24kN we hypothesise that each bolt hole in the CSK joint sustains approximately equal amounts of bearing damage area, indicated by the first dashed circles around the bolt holes in Figure 10. Then, Bolt 1 fails suddenly and the joint load drops to 14kN. The joint then behaves as a two bolt joint (as Bolts 2 and 3 are still intact) and further progressive damage occurs as the joint reloads to approximately 19kN. During this reloading the damage area increases at Holes 2 and 3 to the second dashed circular area indicated. Bolt 2 then fails suddenly, the joint load drops to approximately 8kN, and Bolt 3 then sustains all the remaining joint load and acts as a single bolt joint. The

joint again reloads to 12kN causing further bearing damage progression at Hole 3, until Bolt 3 fails and catastrophic joint failure occurs. The damage area from the single-bolt joint test in Figure 5 is shown insert in Figure 10, and as can be seen the damage area at Hole 1 when Bolt 1 fails in the three-bolt joint is almost identical to that of the single bolt joint case at failure. Furthermore, the damage at Hole 2 is approximately twice, while at Hole 3 is approximately three times, that of the single bolt damage area. In addition, it should be noted that this first significant failure load in the three bolt joint of 24kN is approximately three times that of the average single bolt failure load of approximately 8.3kN. This simple linear superposition of failure load and damage area suggests that single-bolt joint tests results can be used to predict the response of three-bolt joints with reasonable accuracy. However, much further experimental testing is required to further validate this hypothesis; especially for larger joint assemblies with many more fasteners in two-dimensional straight and staggered arrays and under load (rather than displacement) controlled scenarios.

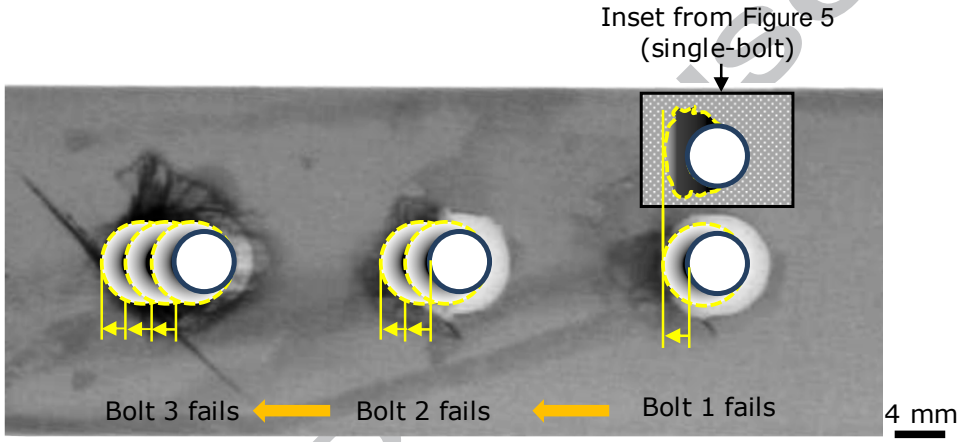

Figure 10: Schematic illustration of damage development in three-bolt countersunk CBJ

4. Conclusions

Comparison of load-displacement data and damage area in single- and three-bolt CBJs provided a detailed insight into the development of damage in countersunk CBJs. Characteristic failure points (A,B,C) and stiffnesses (primary, secondary and tertiary) were featured in the load-displacement curves. This provided an objective insight into the severity of composite damage at a particular load level. It was found that the ultimate failure point 'C' in single-bolt CBJ and the first-bolt-failure point in three-bolt CBJ correspond to the composite plies undergoing intra-laminar damage including extensive fibre buckling and breakage. The size of the damage was approximately reached to the edge of the countersunk head (approx. 4 mm).

The onset point, point A, was shown to be related to the sticking-to-slipping mechanism which, most probably, results in the initiation and propagation of debonding and matrix damage observed at the bottom plies where composite-to-composite friction is present. Point B was identified as the main turning point from the secondary to tertiary stage, contributing to greater than 80% reduction in stiffness in single- and three-bolt CBJ. This, tertiary stage with the highest shear deformation among the three stages, is believed to be the regime where extensive fibre buckling and fibre cluster breakage occurs.

X-ray properly captured bearing damage at holes with a combination of in-plane and intra-laminar delamination damage. Slight inter-laminar delamination and fibre-matrix debonding damage were found the mechanisms occurring away from the holes. Figure 11 schematically shows the mechanism and extension of damage. Summarising from the single- and three-bolt CBJ optical and X-ray images, the most possible failure modes occur as follows: Ply damage occurs underneath the countersunk head due to the compressive stress, properly captured by X-ray. The ply damage extends to the opposite direction of the loading direction, and through-the-thickness. Slight inter-laminar delamination occurs beyond this region, mostly occurring between the middle plies. Slight transverse damage follows the delamination, kinking through the 45° plies. Fibre-matrix debonding is relatively extensive. While delamination dissipates energy in the middle plies, debonding mostly occurs at the bottom.

Finally, a new design rule was developed based on the experiemental studies of damage area and the linear superposition of failure load to estimate damage area and predict the response of a multi-bolt CBJ. The scheme uses the single-bolt joint tests results as an intial baseline. It then suggests that the first bolt in the three-bolt CBJ fails when the damage underneath the countersunk head at all three holes reaches to that in the single-bolt one. This damage area is then added to the remaining holes until the second bolt fails, and so on for the remaining holes. Hereby, the scheme provides a quick, efficient and simplified tool for joining design applications.

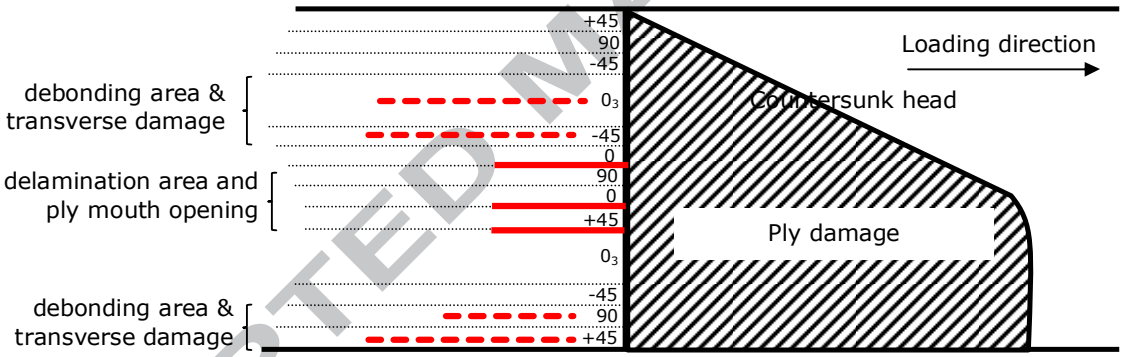

Figure 11: Schematic illustration of dominant failure modes and their locations in CSK part of CBJs; solid and dashed lines represent delamination and debonding/transverse dominant area respectively, with the length representing their schematic extension

Acknowledgments

The research leading to these results has received funding from the European Community's Seventh Framework Programme FP7/2007-2013 under grant agreement nº213371 (MAAXIMUS, www.maaximus.eu) and Science Foundation Ireland (grant 13/IA/1833) for the project of Fastener-less Joining Technologies for High Performance Hybrid Composites-Metal Structure (FALCOM).

References

1. Zhou, Y., et al., *A three dimensional implicit finite element damage model and its application to single-lap multi-bolt composite joints with variable clearance.* Composite Structures, 2015. **131**: p. 1060-1072.
2. Zhou, Y.H., et al., *A study of intra-laminar damage in double-lap, multi-bolt, composite joints with variable clearance using continuum damage mechanics.* Composite Structures, 2014. **116**: p. 441-452.
3. Egan, B., et al., *Static and high-rate loading of single and multi-bolt carbon-epoxy aircraft fuselage joints.* Composites Part a-Applied Science and Manufacturing, 2013. **53**: p. 97-108.
4. Pearce, G.M., et al., *Experimental Investigation of Dynamically Loaded Bolted Joints in Carbon Fibre Composite Structures.* Applied Composite Materials, 2010. **17**(3): p. 271-291.
5. Pearce, G.M., et al., *Numerical Investigation of Dynamically Loaded Bolted Joints in Carbon Fibre Composite Structures.* Applied Composite Materials, 2010. **17**(3): p. 329-346.
6. Pearce, G., *High strain-rate behaviour of bolted joints in carbon fibre composite structures, PhD Thesis*. 2009: School of Mechanical and Manufacturing Engineering, University of New South Wales, Sydney, Australia.
7. McCarthy, M.A., et al., *Three-dimensional finite element analysis of single-bolt, single-lap composite bolted joints: part I - model development and validation.* Composite Structures, 2005. **71**(2): p. 140-158.
8. Camanho, P.P. and F.L. Matthews, *Delamination onset prediction in mechanically fastened joints in composite laminates.* Journal of Composite Materials, 1999. **33**(10): p. 906-927.
9. Nezhad, H.Y., et al., *Numerical analysis of low-velocity rigid-body impact response of composite panels.* International Journal of Crashworthiness, 2015. **20**(1): p. 27-43.
10. Yazdani Nezhad, H.A., A.McCarthy, C.O'Higgins, R., *Impact Damage Response of Carbon Fibre-reinforced Aerospace Composite Panels*, in *20th International Conference on Composite Materials*. 2015: Copenhagen, Denmark.
11. McCarthy, M.A., et al., *Bolt-hole clearance effects and strength criteria in single-bolt, single-lap, composite bolted joints.* Composites Science and Technology, 2002. **62**(10-11): p. 1415-1431.
12. McCarthy, M.A., C.T. McCarthy, and G.S. Padhi, *A simple method for determining the effects of bolt-hole clearance on load distribution in single-column multi-bolt composite joints.* Composite Structures, 2006. **73**(1): p. 78-87.
13. Gray, P.J., R.M. O'Higgins, and C.T. McCarthy, *Effects of laminate thickness, tapering and missing fasteners on the mechanical behaviour of single-lap, multi-bolt, countersunk composite joints.* Composite Structures, 2014. **107**: p. 219-230.
14. Gray, P., R. O'Higgins, and C.T. McCarthy, *Synthesis report on validation tests for manufacturing effects, MAAXIMUS-WP6.5-ULIM-CTD6.5.4*. 2011.
15. *ASTM D5961/D5961M, Standard Test Method for Bearing Response of Polymer Matrix Composite Laminates*. 1996.
16. McCarthy, C.T., M.A. McCarthy, and V.P. Lawlor, *Progressive damage analysis of multi-bolt composite joints with variable bolt-hole clearances.* Composites Part B-Engineering, 2005. **36**(4): p. 290-305.
17. Lawlor, V.P., M.A. McCarthy, and W.F. Stanley, *An experimental study of bolt-hole clearance effects in double-lap, multi-bolt composite joints.* Composite Structures, 2005. **71**(2): p. 176-190.

Bearing damage characteristics of fibre-reinforced countersunk composite bolted joints subjected to quasi-static shear loading

Yazdani Nezhad, Hamed

2017-01-16

Hamed Yazdani Nezhad, Brian Egan, Fiachra Merwick, Conor T. McCarthy, Bearing damage characteristics of fibre-reinforced countersunk composite bolted joints subjected to quasi-static shear loading, Composite Structures, Volume 166, 15 April 2017, pp184-192

http://dx.doi.org/10.1016/j.compstruct.2017.01.029